JOURNAL OF VIROLOGY, June 2002, p. 5720–5728 Vol. 76, No. 11
0022-538X/02/$04.00+0 DOI: 10.1128/JVI.76.11.5720–5728.2002

Measles Virus Spreads in Rat Hippocampal Neurons by Cell-to-Cell Contact and in a Polarized Fashion

Markus U. Ehrengruber,[1] Elisabeth Ehler,[2] Martin A. Billeter,[3] and Hussein Y. Naim[3]*

Brain Research Institute[1] and Institute of Molecular Biology,[3] University of Zurich, CH-8057 Zurich, and Institute of Cell Biology, Swiss Federal Institute of Technology, CH-8093 Zurich,[2] Switzerland

Received 14 December 2001/Accepted 1 March 2002

Measles virus (MV) can infect the central nervous system and, in rare cases, causes subacute sclerosing panencephalitis, characterized by a progressive degeneration of neurons. The route of MV transmission in neurons was investigated in cultured rat hippocampal slices by using MV expressing green fluorescent protein. MV infected hippocampal neurons and spread unidirectionally, in a retrograde manner, from CA1 to CA3 pyramidal cells and from there to the dentate gyrus. Spreading of infection depended on cell-to-cell contact and occurred without any detectable release of infectious particles. The role of the viral proteins in the retrograde MV transmission was determined by investigating their sorting in infected pyramidal cells. MV glycoproteins, the fusion protein (F) and hemagglutinin (H), the matrix protein (M), and the phosphoprotein (P), which is part of the viral ribonucleoprotein complex, were all sorted to the dendrites. While M, P, and H proteins remained more intracellular, the F protein localized to prominent, spine-type domains at the surface of infected cells. The detected localization of MV proteins suggests that local microfusion events may be mediated by the F protein at sites of synaptic contacts and is consistent with a mechanism of retrograde transmission of MV infection.

Measles virus (MV) has a nonsegmented negative-strand RNA genome and belongs to the family *Paramyxoviridae*. The virus envelope contains two transmembrane glycoproteins, a fusion protein (F) and hemagglutinin (H), whereas matrix protein (M) interacts with both the envelope and the helical ribonucleoprotein (i.e., the viral genome encapsulated by N and P proteins) to form the virion (18). Measles is one of the leading causes of childhood mortality in the world, primarily due to strong MV-induced immunosuppression favoring secondary infections (39). Encephalomyelitis occurs occasionally during the acute phase of MV infection, while subacute sclerosing panencephalitis (SSPE), a rare sequel of central nervous system infections, occurs many years later (42).

SSPE is characterized by a slow progressive deterioration of the brain. Infection proceeds despite the presence of a high level of neutralizing antibody in the cerebrospinal fluid (43). It is suggested that MV spreads transneuronally to the brain (35, 44). Usually, recovery of infectious units from SSPE patient brain requires cocultivation with permissive fibroblasts (2). Virions recovered by this method carry various mutations, particularly in the F and M genes (3), that apparently enhance cell-to-cell fusion (7, 8).

Transgenic mice expressing human CD46 (33, 35), the receptor for the Edmonston B strain of MV, have been employed to study MV neuropathology. In these mice, MV infects the brain and causes neuronal apoptosis (12, 28), and in primary cultures of hippocampal neurons MV efficiently propagates with little extracellular release of infectious units (37). Rat neuronal cultures, however, efficiently release infectious units when a neuroadapted MV strain is used (25). Whereas neuropathological studies show a clear interaction of MV with the central nervous system, the mechanism of MV transmission within the brain remains obscure.

In contrast to that in neurons, MV propagation in epithelial cells is well understood. An essential role for M protein in MV assembly and shedding was found previously (34). M protein is required for the apical release of infectious particles (4, 27, 34) and for the apical sorting of the envelope glycoproteins F and H (34). Similar to epithelial cells, neurons are also polarized and sort proteins to dendrites, axons, or both (5). Studies with vesicular stomatitis virus and avian influenza-fowl plague virus suggest that epithelial cells and neurons share common features for the sorting of proteins to the apical surface and axons or to the basolateral surface and dendrites, respectively (11).

Here, we investigated transmission and protein sorting of MV in hippocampal neurons. We used cultured rat hippocampal slices in which neurons retain normal morphology and synaptic connections (17). To visualize the progression of MV infection, we utilized a replication-competent MV expressing green fluorescent protein (GFP).

MATERIALS AND METHODS

Preparation of recombinant MV. Recombinant MV of the Edmonston B strain expressing enhanced GFP (eGFP; Clontech) was recovered from pMeGFPNV by using the 293-3-46 rescue cell line, which stably expresses the T7 RNA polymerase and the N and P proteins of MV (36). The eGFP cDNA was cloned as a single transcription unit upstream of the N protein gene (19). MV-GFP was propagated in Vero cells and had a titer of 1×10^6 to 2×10^6 PFU/ml.

Infection of slice cultures and analysis of GFP expression. Hippocampal slices from 6-day-postnatal rats were cultured in the roller-tube configuration (17). At 7 to 21 days in vitro, slice cultures (12.7 ± 1.4 days in vitro, 10 batches; 2 to 30 cultures/batch) were injected with ~0.2 μl of virus over four to six sites in the CA1 or CA3 region or with ~0.4 μl over 8 to 12 sites in both the CA1 and CA3 regions as described previously (14, 15). Briefly, the infections were performed at room temperature under biosafety containment level 2 conditions by microin-

* Corresponding author. Mailing address: Institute of Molecular Biology, University of Zurich, Winterthurerstrasse 190, CH-8057 Zurich, Switzerland. Phone: (41 1) 635 3112. Fax: (41 1) 635 6864. E-mail: naim@molbio.unizh.ch.

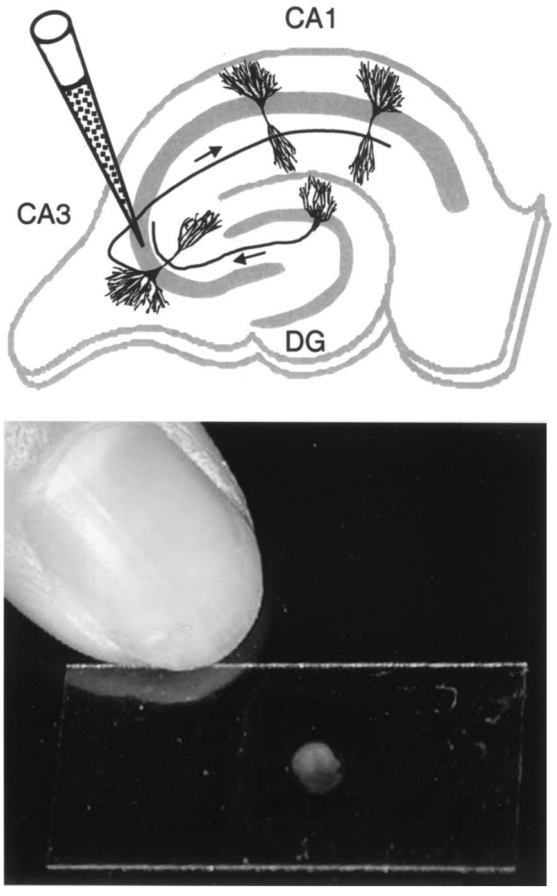

FIG. 1. Infection of hippocampal slices. (Top) Schematic representation of a hippocampal slice with the locations of CA1 and CA3 pyramidal cells and of a granule cell in the dentate gyrus (DG). The position of a glass micropipette, which contains the viral solution, inserted into the pyramidal cell layer (as indicated by the gray area) of the CA3 region is indicated. Arrows along the axons indicate the unidirectional progression of excitatory pathways, with mossy fibers from granule cells synapsing onto dendrites from CA3 pyramidal cells and Schaffer collaterals from CA3 pyramidal cells connecting to dendrites from CA1 pyramidal cells. Note that granule cells are presynaptic to CA3 pyramidal cells, which themselves are presynaptic to CA1 pyramidal cells, whereas this is normally not the case for the reverse. (Bottom) Photograph of a rat hippocampal slice cultured on a 12- by 24-mm glass coverslip.

jection of virus into the extracellular space of the slice cultures. The tip of autoclaved micropipettes, pulled from borosilicate glass (Clark Electronical Instruments, Reading, England), was broken to a diameter of ~20 μm. Pipettes were filled with MV solution and, by using a micromanipulator (Narishige, East Meadow, N.Y.), placed into either the CA1 or CA3 pyramidal cell layer (Fig. 1). For each placement, one short injection (<2 s) was performed by applying pressure from a 1-ml syringe. Immediately upon virus injection, several slices (as indicated) were physically cut with a sterile razor blade to separate the injected CA1 region from the rest of the slice. Subsequent microscopic examination revealed that in some cases the CA1 region was not completely separated; these slices were therefore considered partially cut.

Slices were cultured for 35 days postinjection (dpi), and living slices were analyzed and photographed in their roller tubes. Cell viability was tested by propidium iodide (5 μg/ml) exclusion. All slices were viewed with an inverted Axiovert 100 microscope (Zeiss, Feldbach, Switzerland) and photographed with an upright Axioplan fluorescence microscope (Zeiss). GFP fluorescence was observed with a fluorescein isothiocyanate filter set (Zeiss) with band-pass filters of 450 to 490 and 515 to 565 nm for excitation and emission, respectively. Propidium iodide fluorescence was observed with a rhodamine filter set (Zeiss) with a 540- to 552-nm band-pass filter for excitation and a 590-nm long-pass filter for emission.

Immunocytochemistry and confocal microscopy. Slices were fixed with 4% (wt/vol) paraformaldehyde (Fluka, Buchs, Switzerland) in phosphate-buffered saline (PBS) for ~12 h at 4°C in the dark, washed with PBS, and processed for immunocytochemistry as described previously (30). Briefly, slices were permeabilized at room temperature for 12 h in PBS containing 0.4% Triton X-100 (to allow permeabilization through the slice and glial cells covering it) and blocked for 1 h with PBS containing 1% (vol/vol) heat-inactivated horse serum. Slices were then incubated for 4 days at 4°C with monoclonal anti-F, -H, -M, or -P antibodies (20, 34) at a dilution of 1:300 in PBS. Three consecutive washings with PBS were performed at room temperature, for 30 min each. Secondary goat anti-mouse immunoglobulin G antibodies coupled to Cy3 or Texas red were applied at a dilution of 1:200 in PBS to the slices for 3 h at room temperature. After six PBS washings, 30 min each, slices were mounted onto microscope slides and visualized by confocal microscopy as previously described (34).

Statistical analysis. Data are expressed as means ± standard errors of the means. For the statistical evaluation of the effect of cutting the CA1 region on the spread of MV, a nonparametric Kruskal-Wallis test was applied. The Mann-Whitney test was used for the statistical evaluation of anterograde versus retrograde spread of MV in intact slices. Nonparametric Wilcoxon signed-rank tests were performed to statistically examine the transmission of MV into the different hippocampal areas. The statistical software Statview 4.0 (SAS Institute, Cary, N.C.) was used for all analyses.

RESULTS

MV propagates in rat hippocampal neurons. We injected ~100 to 200 PFU of MV-GFP particles into the CA1 or CA3 region of hippocampal slices at 12.7 ± 1.4 days in culture, i.e., at a time when the synapses in this system have matured (29), and evaluated the propagation of MV-GFP at several time points. GFP-positive pyramidal cells, interneurons, and glial cells, identified by their characteristic morphology and location within the slice, were found as early as 1 dpi. The percentage of GFP-positive pyramidal cells increased significantly ($P < 0.001$, chi-square test) with time, from 60% of all GFP-positive cells at 3 dpi to 95.7% at 14 dpi, while the fraction of GFP-positive interneurons remained roughly constant (0.8 and 1.0% at 3 and 14 dpi, respectively). Figure 2A shows that the number of GFP-positive cells increased from 21 ± 6 cells per slice at 3 dpi to 294 ± 30 cells per slice at 14 dpi; Fig. 2B and C illustrate the finding that the vast majority of newly infected cells were pyramidal cells. Similar results were obtained with cultures injected with 5 to 10 PFU of MV-GFP per slice.

We examined cell survival by assaying for propidium iodide exclusion. At 17 dpi, >90% of the GFP-positive pyramidal cells excluded propidium iodide (Fig. 2C and D). At all times after infection, cell-to-cell fusion and syncytium formation (leading to multinucleated neurons) were never observed. In addition, electrophysiological recordings performed on GFP-positive CA1 pyramidal cells from slices at 9 to 10 dpi had revealed normal excitability in MV-GFP-infected neurons (13). These data suggest that infected pyramidal cells remained intact and viable up to 17 dpi. As rat hippocampal neurons are devoid of the receptor (CD46) for the MV strain used, it appears that the mechanism of MV spread in hippocampal neurons is different from that in epithelial cells or fibroblasts expressing CD46.

Polarity of MV transmission. To determine the route of MV transmission in hippocampal slices, we selectively injected MV into the CA1 or CA3 region and monitored MV transmission at regular intervals (up to 25 days).

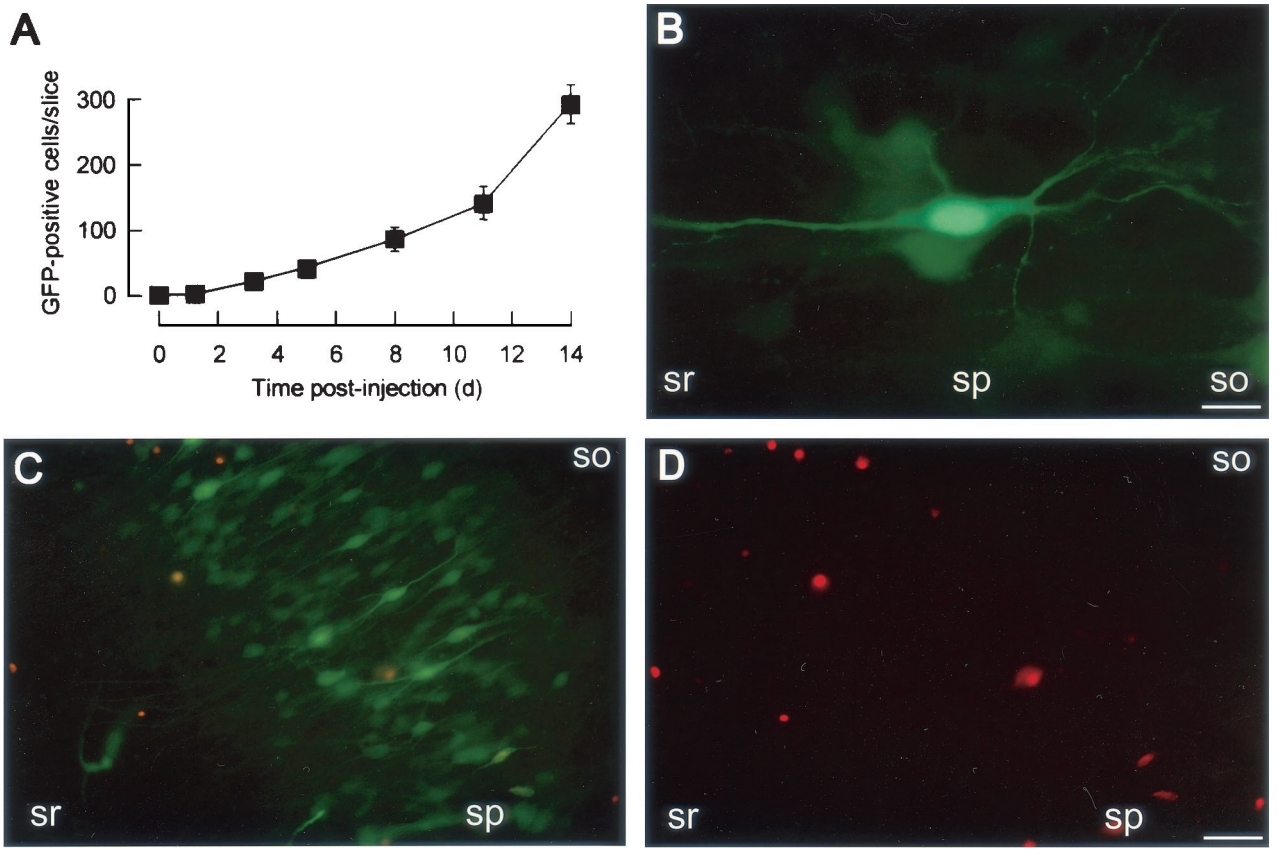

FIG. 2. MV spreads in cultured hippocampal slices. (A) Time course of MV transmission. Nine slices were injected with ~100 infectious MV-GFP particles, and the number of GFP-positive cells per slice was determined at increasing time intervals. (B) High-magnification fluorescence micrograph of a GFP-positive CA1 pyramidal cell from a slice at 9 days after MV-GFP application. (C) Fluorescence micrograph of the CA3 region from a living slice injected with MV-GFP and stained with propidium iodide at 17 dpi. A fluorescein isothiocyanate filter set was used (see Materials and Methods); GFP fluorescence (green) shows MV-infected cells, whereas propidium iodide fluorescence (red) indicates nonviable cells. (D) Propidium iodide fluorescence micrograph of the same region as in panel C with a rhodamine filter set. Abbreviations: so, stratum oriens; sp, stratum pyramidale; sr, stratum radiatum. Bars, 20 μm (B) and 65 μm (C and D).

CA1 infection. In 24 slices in which MV-GFP was injected into the CA1 region, GFP fluorescence spread readily to the CA3 pyramidal cell layer at 4 to 6 dpi. After ~13 days, the infection reached the granule cells of the dentate gyrus (Fig. 3A; Table 1). A quantitative analysis of GFP fluorescence spread revealed that initial infection of CA3 pyramidal cells was detected after 5.6 ± 1.0 days and that infection of granule cells was detected at 13.0 ± 1.3 dpi (Table 1). The number of infected CA3 pyramidal cells increased with time, reaching >100 cells at 13.0 ± 1.7 dpi (Table 1). These results strongly suggest that MV spreads from CA1 pyramidal cells to CA3 pyramidal cells and from there to granule cells.

CA3 infection. In 16 slices in which MV-GFP was injected into the CA3 region, GFP fluorescence spread readily between CA3 pyramidal cells and to granule cells of the dentate gyrus (Fig. 3B). Compared to CA1 injections, MV reached the granule cells much faster, i.e., at 3.2 days after MV injection (Table 1). Interestingly, propagation of MV-dependent GFP fluorescence from the CA3 to the CA1 region was inefficient (Fig. 3B). Only after 17 dpi were a few GFP-positive CA1 pyramidal cells observed. Transmission to the CA1 region was generally confined to areas close to the CA3 region (<25 GFP-positive cells [Table 1]). Compared to the spread of GFP from CA1 to CA3 pyramidal cells, the propagation of GFP from the CA3 region to CA1 pyramidal cells was significantly slower (17.8 ± 1.3 versus 5.6 ± 1.0 days [Table 1]).

For the hippocampal slice preparation used, Debanne et al. have previously shown that there is a high (76%) probability for a CA3 pyramidal cell to innervate a CA1 pyramidal cell and a low (8%) probability for the reverse functional coupling of CA1 to CA3 pyramidal cells, whereas both CA1 and CA3 pyramidal cells form synaptic contacts among themselves (10). In addition, in hippocampal slice cultures, granule cells innervate CA3 but not CA1 pyramidal cells (47). Our results for the directional spreading of MV in hippocampal slices thus correlate with the pattern of synaptic connectivity of pyramidal cells and granule cells and suggest that MV propagates in a unidirectional, retrograde fashion across hippocampal neurons.

MV spreads by cell-to-cell contact. Our observation that MV-dependent GFP fluorescence propagates to principal neurons and spreads unidirectionally indicates that infection is transmitted by cell-to-cell contact. In order to test this hypothesis, the injected CA1 regions in six slices were completely cut off from the rest of the tissue immediately upon the application

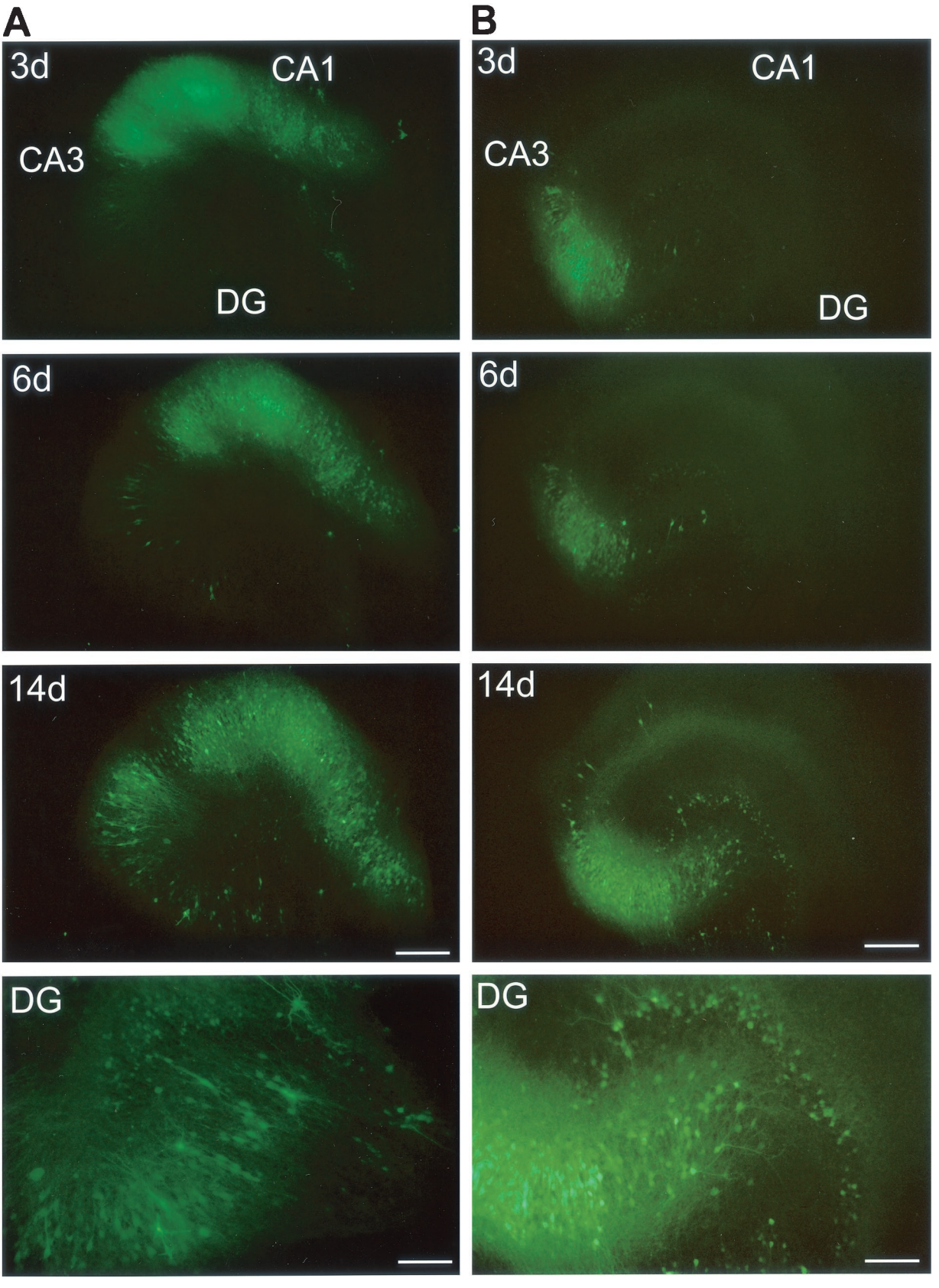

FIG. 3. Polarity of MV transmission. Injection of MV-GFP into the CA1 region (A) results in the propagation of MV to the CA3 region and dentate gyrus (DG), whereas injection of MV-GFP into the CA3 region (B) results in transmission to the dentate gyrus but only inefficiently to the CA1 region. Fluorescence micrographs at 3, 6, and 14 dpi are shown; bottom panels (DG) show a magnification of the dentate gyrus at ~14 dpi. The DG panel of the CA1-injected slice (A) shows a magnification that is rotated by 50° counterclockwise with regard to the upper panels and is exposed longer to better visualize GFP-positive granule cells. Bars, 20 μm (3-, 6-, and 14-day panels) and 80 μm (DG panels).

TABLE 1. Spreading pattern of MV in hippocampal slices[a]

Injection site	*n* (slices)	Initial spread[b] (days) to:		Extensive spread[c] (days) to CA1 or CA3
		CA1 or CA3	Dentate gyrus	
CA3	10	17.8 ± 1.3[e]	3.2 ± 0.2[f,g]	24.3[d,e]
CA1 (slice intact)	11	5.6 ± 1.0	13.0 ± 1.3[g]	13.0 ± 1.7
CA1 (partial cut)	5	6.2 ± 0.4	15.3 ± 2.7[g]	15.0 ± 1.0
CA1 (slice cut)	6	>25	>25	>25

[a] Values for spread are means ± standard errors of the means after injection of MV into the indicated site (analysis ended at 25 days). For completely cut slices, a Kruskal-Wallis test revealed a statistically significant effect ($P < 0.01$) of cutting (compare with Fig. 4) on the initial and extensive spread of MV to CA3 and the dentate gyrus. For intact slices, MV reached the dentate gyrus faster upon CA3 injection than upon CA1 injection, and a Wilcoxon signed-rank test revealed that in CA1-injected slices MV spreads first to CA3 and then to the dentate gyrus. In CA3-injected slices MV spreads to the dentate gyrus before CA1. Most importantly, anterograde spread of MV from CA3 to CA1 is much slower than retrograde spread from CA1 to CA3.

[b] Initial spread is defined by ≤25 GFP-positive neurons in the indicated region.

[c] Extensive spread is defined by ≥100 GFP-positive neurons in the indicated region.

[d] Note that for CA3-injected slices only 1 out of 10 slices showed extensive spread (at 18 days postinfection), while no extensive spread was detected in the remaining nine slices even 25 days after the MV injection (i.e., the time point when the analysis was ended).

[e] $P = 0.002$ (Mann-Whitney test).

[f] $P < 0.001$ (Mann-Whitney test).

[g] $P < 0.05$ (Wilcoxon signed-rank test).

of MV-GFP. As expected, GFP did not propagate from the separated CA1 areas to the neighboring CA3 region or dentate gyrus (Fig. 4; Table 1). In five cultures in which the injected CA1 region was only partially separated from the rest of the slice, transmission of GFP from the CA1 to the CA3 region and dentate gyrus was observed with an average delay of 0.6 to 2.3 days (Table 1). As the hippocampal slices were kept in the roller-tube configuration (17), the culture medium was under continuous rotation, implying that—if MV was released as free particles—other cells within the same culture should be randomly infected. But this did not occur, either in the intact tissue or in the cut tissue, proving that MV does not bud as free particles from hippocampal slices. This conclusion corresponds to similar findings for dissociated hippocampal neurons and in vivo (12, 24). Moreover, the physical separation of the CA1 region was done to destroy the synaptic connections between the CA1 and CA3 region, which concomitantly prevented MV from spreading from the CA1 to the CA3 region (and the dentate gyrus). Our results obtained with cut slices thus support the previous experiments whose results are shown in Fig. 3.

To ascertain whether hippocampal slices liberate free MV particles, culture media of infected slices were plaque assayed on Vero cells. As expected, no MV infectivity was recovered from the culture medium of 12 GFP-positive slices at up to 14 days after injection of MV-GFP into the CA1 or CA3 region, or both. Titers shed from infected slices and cultured epithelial (CaCo2) and fibroblast (Vero) cells, used as controls, were compared. In contrast to the hippocampal slices, CaCo2 and Vero cells infected with a total of 100 or 1,000 plaque-forming MV-GFP particles released considerable numbers of infectious units (0.8×10^4 to 1.6×10^4 or 2.0×10^4 to 6.0×10^4 PFU, respectively) at a time point when >50% of the CaCo2 and Vero cells were GFP positive. As our slice cultures were coated with chicken plasma, released virions might have been trapped under this layer, and therefore, virion release into the slice culture medium might have been hindered. In order to test this possibility, two batches of six slices were homogenized at 6 to 14 dpi, and the homogenates were centrifuged and assayed on Vero cells. Again, no release of MV infectivity was detected. Taken together, these results demonstrate that MV spreads between pyramidal cells by cell-to-cell contact rather than by released infectious particles.

Sorting of the envelope and matrix proteins in infected pyramidal cells. The results presented above show that MV is transmitted in a retrograde fashion, independent of the release of infectious particles. The viral envelope proteins, F and H, could support the observed polarized MV transmission in neurons because they are the key players in mediating cell-to-cell fusion (46). On the other hand, M protein plays a crucial role in regulating glycoprotein sorting and virus release in polarized epithelial cells (34). Since neurons are also polarized, we investigated the sorting of F, H, and M proteins by immunofluorescence and confocal microscopic analysis. Figure 5A illustrates the localization of F protein in GFP-positive CA3 pyramidal cells. F protein was sorted to dendrites (Fig. 5A, middle panel) and concentrated in small patches, possibly spines, at the surface of soma and dendrites (Fig. 5A, right panel). H protein was also localized to dendrites of GFP-positive CA3 pyramidal cells (Fig. 5B, middle panel), but compared to the F protein, H protein was not highly concentrated on the surface of dendrites or spine-like structures (Fig. 5B, right panel). Because the localization patterns of F and H were reproducibly different in three independent experiments (six slices each), these findings indicate that the transport of F and H proteins in neurons is different from that in polarized epithelial cells.

The sorting of M protein in infected CA3 pyramidal cells was also determined (Fig. 5C). M protein was restricted to intracellular domains of the somatodendritic compartment (Fig. 5C, middle panel). As M protein localized to dendrites, we conclude that, in contrast to polarized epithelial cells (34), it did not affect the natural sorting pattern of envelope glycoproteins in pyramidal cells.

The expression of F, H, and M proteins was detected at sites distant from MV injection sites (in CA3 and dentate gyrus, when MV was injected into CA1). This may indicate that the MV genome has propagated from the originally infected cell to neighboring cells and that de novo gene expression has occurred (Fig. 5). To ascertain that not only viral mRNAs or proteins but indeed the viral genome is transmitted from CA1 to CA3 pyramidal cells, we examined the expression of P protein (which is associated with the viral ribonucleoprotein) in CA3 regions of slices infected only in the CA1 region. Figure 5D shows that the GFP-positive CA3 pyramidal cells (left panel) exhibited P protein immunoreactivity (middle panel). In MV-infected cells, P protein is mainly localized in ribonucleoprotein clusters, whereas heterologous expression of the P protein alone causes a diffuse, cytosolic distribution (20). Thus, in our slice cultures, the P protein was most likely associated with viral ribonucleoprotein, suggesting that the MV genome has been transmitted from CA1 to CA3 pyramidal cells.

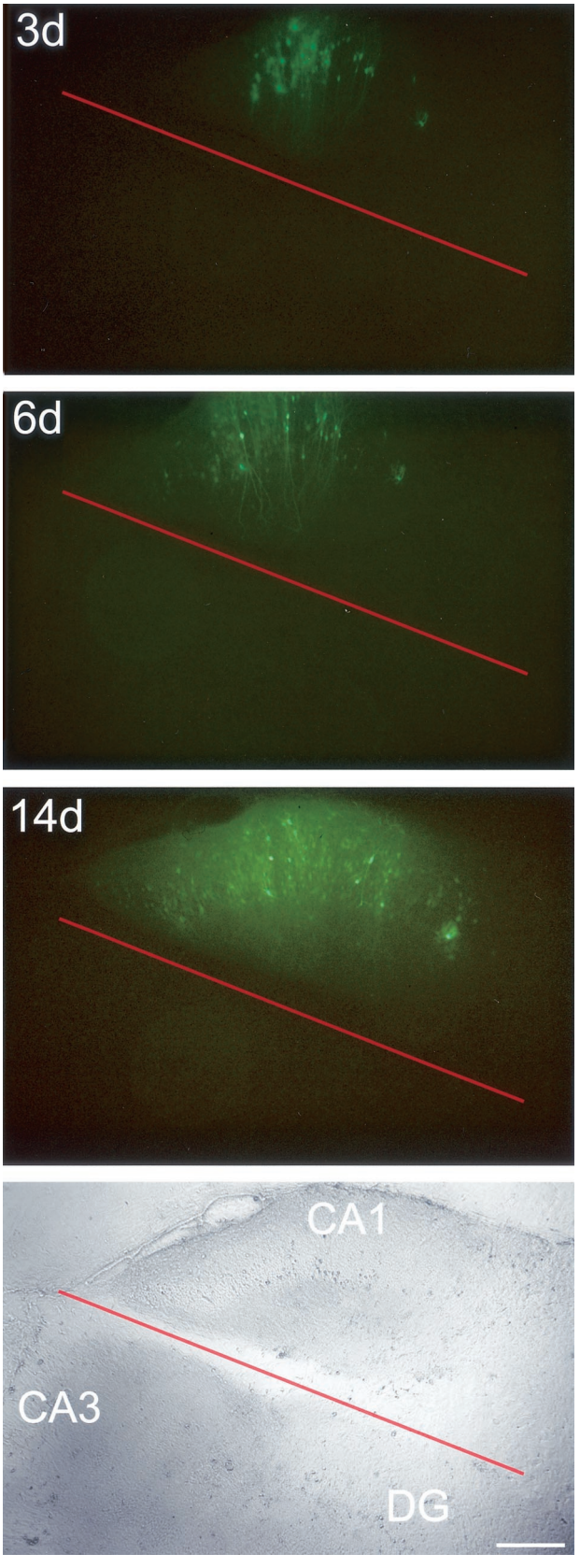

FIG. 4. Separation of the MV-injected CA1 region prevents MV spread to the CA3 region and dentate gyrus (DG). Fluorescence (top) and bright-field (bottom) micrographs at 3, 6, and 14 dpi of a slice for which MV-GFP was applied to the CA1 region and the injected region was separated (red line) immediately thereafter. Bar, 320 μm.

DISCUSSION

In this study we demonstrate that in neurons of hippocampal slices MV efficiently spreads, not by the release of extracellular virus or by syncytium formation, but retrogradely by localized cell-to-cell contact at synapses. Since rat brain is devoid of the human CD46 receptor or its homologue (32), it is remarkable that infection of rat hippocampal tissue occurs in the apparent absence of CD46. The initial penetration of MV into hippocampal neurons could be due either (i) to the mode of inoculation (injection into slices), which could mechanically introduce virus into cells, or (ii) to alternative receptors or CD46 homologues present on immature rat neurons. The first possibility is unlikely because MV, unlike other viruses (which are taken up by the endosomal pathway), must fuse at the cell surface and not intracellularly to promote infection. The second possibility is supported by the fact that MV can infect murine cells (12) and brains of neonatal rats (for a review, see reference 26) and (upon passaging from one neonatal brain to another) can adapt to efficiently infect adult rat brains, suggesting that immature rat neurons possess alternative receptors that can be used by MV.

The mode of MV spread in neurons from rat hippocampal slices agrees with the conclusions of Rall and colleagues (24), who showed that MV can spread in cultures of dissociated hippocampal neurons from CD46-transgenic mice in the presence of anti-CD46 antibodies that inhibit MV binding and infection. The fact that, in contrast to CaCo2 and Vero cells, infected hippocampal neurons both in vitro and in situ do not release infectious MV particles strongly suggests that in nervous tissue MV does not follow the classical route of infection. We thus conclude that in hippocampal neurons MV assembly is deficient and that the virus is transmitted by cell-to-cell contact. In support of this conclusion, it has been previously shown that MV can spread from persistently infected, nonneuronal cells to neighboring cells in a contact-dependent manner (16, 31, 34). Other support comes from the findings of Duprex et al., who demonstrated, by employing the same MV expressing GFP as used in this study, that infection in human and murine neuroblastoma cells spreads by cell-to-cell contact along pathways (12). Interestingly, we found MV to propagate to neurons rather than glial cells. Thus, our results and the former reports using different systems support the hypothesis that interneuronal viral transmission occurs via synapses.

The spread of MV infection requires that ribonucleoprotein be transferred from one infected neuron to another. It has been shown previously that F protein requires H protein to trigger extensive cell-to-cell fusion (8, 46). The lack of H protein on the surface of spine-like structures from dendrites and soma (Fig. 5A and B) explains the absence of syncytium formation in the brain tissue. However, this does not exclude the possibility that F protein could promote microfusions, either alone, at sites where it is concentrated, or with the help of minor amounts of H protein (not detectable by our confocal techniques) localized at these sites. It is, therefore, likely that infectious ribonucleoprotein translocates via such microfusions

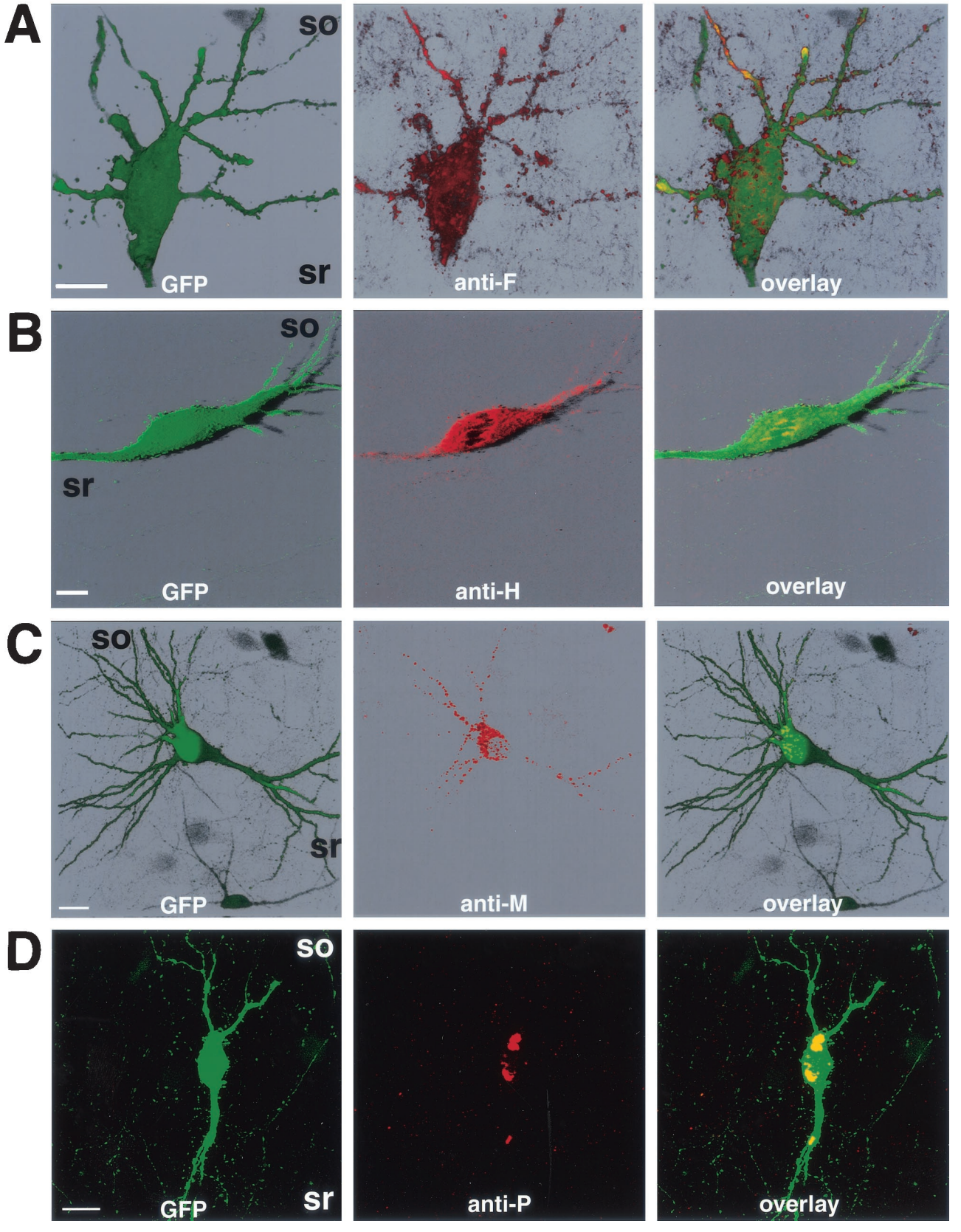

FIG. 5. Localization of F (A), H (B), M (C), and P (D) proteins in infected CA3 pyramidal cells. Slices were fixed at 7 dpi, permeabilized, and incubated with monoclonal antibodies directed against F, H, M, or P proteins (middle panels of A to D, respectively). F, H, and M protein localization is shown by three-dimensional reconstitution (A to C); P protein localization is shown by extended focus of plane images (D). Note that only GFP-positive neurons were reactive toward the antibodies used. Abbreviations: so, stratum oriens; sr, stratum radiatum. Bars, 20 μm.

at synapses. Such a mode of transmission requires no release of infectious particles and is in line with the fact that infectious virions could not be recovered from the brains of SSPE patients (25). It may, therefore, represent the natural route of MV transmission within the brain.

Our data demonstrate that viral envelope proteins and ribonucleoproteins are sorted to dendrites. These findings are consistent with those of an electron microscopic study of MV-infected mouse brain, which showed that MV ribonucleoprotein was aligned along postsynaptic endings (45), and suggest retrograde MV transmission. Since, in addition, (i) it is known that 76% of the axons from CA3 pyramidal cells form synapses onto a given CA1 pyramidal cell whereas only 8% of the CA1 pyramidal cell axons form synapses onto a given CA3 pyramidal cell (10) and (ii) we show that MV spreads much more efficiently from the CA1 to the CA3 region than in the reverse direction (Fig. 3; Table 1), MV appears to spread in an exclusively retrograde manner.

Based on the present data, the sorting of MV proteins in epithelial cells and that in neurons are different. In epithelial cells, the envelope glycoproteins F and H are targeted intrinsically to the basolateral domain, but M protein retargets a large percentage of F and H protein to the apical domain (34). Here, in neurons, M protein is not required for the formation of infectious particles, and M protein does not retarget F and H proteins from dendrites to axons, as would be expected if the analogy to polarized epithelial cells (11, 34) were correct. Moreover, we show that the F protein, but not the H protein, is enriched at the dendritic surface, indicating a differential transport of F and H proteins in neurons. It appears that functional F rather than H protein is required for neuronal MV propagation as (i) MV isolated from the brain autopsy samples of SSPE victims forms F proteins with highly conserved, functional ectodomains (required for fusion) and highly altered cytoplasmic tails, whereas the M protein is either absent or highly compromised (1); (ii) due to steep mRNA expression gradients, the ratio of F and H protein is considerably increased in SSPE patient brains (40); and (iii) mutations (deletions or other alterations) were always found in the cytoplasmic tail of F protein from SSPE patient isolates, improving the fusogenic function of the F protein (7). It thus appears that only functional F protein is needed for MV transmission in the brain. Moreover, interactions between the envelope glycoproteins themselves and with the M protein may not be required in neurons and even appear deleterious for efficient MV transmission in the brain. Thus, mutations abolishing or minimizing such interactions, especially in the M and H proteins, might be of selective advantage for MV spread in the central nervous system.

Finally, synapse-specific retrograde spreading has been previously shown for the Bartha strain of pseudorabies virus (6, 41) and for rabies virus (9, 22). Due to this feature, pseudorabies virus has been successfully employed to trace neuronal circuits in rats (21, 23, 38). Our results now suggest that, at least in vitro, MV can be utilized in neuroanatomical studies. In this context, it is interesting that under our conditions MV propagates to pyramidal cells rather than interneurons or glial cells. We have previously shown that MV—compared to the more neurotropic Semliki Forest virus—does not show such a high preference for neurons during the initial infection of hippocampal slices, resulting in 62% of the GFP-positive cells being neurons (13). Here, we now demonstrate that the propagation of MV from originally infected cells to neighboring cells in hippocampal tissue occurs only retrogradely through synapses, i.e., to neurons. In addition, as MV spreads to pyramidal cells, which contain the excitatory neurotransmitter glutamate, rather than to interneurons, which have inhibitory neurotransmitters, it might differentiate between excitatory (glutamatergic) and inhibitory (γ-aminobutyratergic) synapses.

ACKNOWLEDGMENTS

This work was supported by grants 31-57125.99 and 31-45900.95 from the Swiss National Science Foundation to M.U.E. and M.A.B., respectively, and grant 3786.1 from the Commission for Technology and Innovation to M.A.B.

We thank L. Rietschin and L. Heeb for preparing the slice cultures, R. A. McKinney for advice on the immunocytochemistry, J.-C. Perriard for access to the confocal microscope, D. P. Wolfer for help with the statistical analysis, B. H. Gähwiler and U. Gerber for comments on the manuscript, C. Heuss for the schematic representation and E. M. Schneider for the photograph in Fig. 1, and R. Schöb and F. Ochsenbein for help with the photographs.

REFERENCES

1. **Baczko, K., J. Lampe, U. G. Liebert, U. Brinckmann, V. ter Meulen, I. Pardowitz, H. Budka, S. L. Cosby, S. Isserte, and B. K. Rima.** 1993. Clonal expansion of hypermutated measles virus in a SSPE brain. Virology **197:**188–195.
2. **Baczko, K., U. G. Liebert, M. Billeter, R. Cattaneo, H. Budka, and V. ter Meulen.** 1986. Expression of defective measles virus genes in brain tissues of patients with subacute sclerosing panencephalitis. J. Virol. **59:**472–478.
3. **Billeter, M. A., and R. Cattaneo.** 1991. Molecular biology of defective measles viruses persisting in the human central nervous system, p. 323–345. *In* D. Kingsbury (ed.), The paromyxoviruses. Plenum Press, New York, N.Y.
4. **Blau, D. M., and R. W. Compans.** 1995. Entry and release of measles virus are polarized in epithelial cells. Virology **210:**91–99.
5. **Burack, M. A., M. A. Silverman, and G. Banker.** 2000. The role of selective transport in neuronal protein sorting. Neuron **26:**465–472.
6. **Card, J. P., L. Rinaman, J. S. Schwaber, R. R. Miselis, M. E. Whealy, A. K. Robbins, and L. W. Enquist.** 1990. Neurotropic properties of pseudorabies virus: uptake and transneuronal passage in the rat central nervous system. J. Neurosci. **10:**1974–1994.
7. **Cathomen, T., B. Mrkic, D. Spehner, R. Drillien, R. Naef, J. Pavlovic, A. Aguzzi, M. A. Billeter, and R. Cattaneo.** 1998. A matrix-less measles virus is infectious and elicits extensive cell fusion: consequences for propagation in the brain. EMBO J. **17:**3899–3908.
8. **Cathomen, T., H. Y. Naim, and R. Cattaneo.** 1998. Measles viruses with altered envelope protein cytoplasmic tails gain cell fusion competence. J. Virol. **72:**1224–1234.
9. **Coulon, P., C. Derbin, P. Kucera, F. Lafay, C. Prehaud, and A. Flamand.** 1989. Invasion of the peripheral nervous systems of adult mice by the CVS strain of rabies virus and its avirulent derivative AvO1. J. Virol. **63:**3550–3554.
10. **Debanne, D., N. C. Guérineau, B. H. Gähwiler, and S. M. Thompson.** 1995. Physiology and pharmacology of unitary synaptic connections between pairs of cells in areas CA3 and CA1 of rat hippocampal slice cultures. J. Neurophysiol. **73:**1282–1294.
11. **Dotti, C. G., and K. Simons.** 1990. Polarized sorting of viral glycoproteins to the axon and dendrites of hippocampal neurons in culture. Cell **62:**63–72.
12. **Duprex, W. P., S. McQuaid, B. Roscic-Mrkic, R. Cattaneo, C. McCallister, and B. K. Rima.** 2000. In vitro and in vivo infection of neural cells by a recombinant measles virus expressing enhanced green fluorescent protein. J. Virol. **74:**7972–7979.
13. **Ehrengruber, M. U., S. Hennou, H. Büeler, H. Y. Naim, N. Déglon, and K. Lundstrom.** 2001. Gene transfer into neurons from hippocampal slices: comparison of recombinant Semliki Forest virus, adenovirus, adeno-associated virus, lentivirus, and measles virus. Mol. Cell. Neurosci. **17:**855–871.
14. **Ehrengruber, M. U., and K. Lundstrom.** 2000. Alphavirus-mediated gene transfer into neurons, p. 4.22.1–4.22.23. *In* J. Crawley, C. Gerfen, R. McKay, M. Rogawski, D. Sibley, and P. Skolnick (ed.), Current protocols in neuroscience. John Wiley & Sons, New York, N.Y.
15. **Ehrengruber, M. U., K. Lundstrom, C. Schweitzer, C. Heuss, S. Schlesinger, and B. H. Gähwiler.** 1999. Recombinant Semliki Forest virus and Sindbis virus efficiently infect neurons in hippocampal slice cultures. Proc. Natl. Acad. Sci. USA **96:**7041–7046.
16. **Firsching, R., C. J. Buchholz, U. Schneider, R. Cattaneo, V. ter Meulen, and**

J. Schneider-Schaulies. 1999. Measles virus spread by cell-cell contacts: uncoupling of contact-mediated receptor (CD46) downregulation from virus uptake. J. Virol. **73:**5265–5273.
17. **Gähwiler, B. H.** 1981. Organotypic monolayer cultures of nervous tissue. J. Neurosci. Methods **4:**329–342.
18. **Griffin, D. E., and W. J. Bellini.** 1996. Measles virus, p. 1267–1312. *In* B. N. Fields, D. M. Knipe, and P. M. Howley (ed.), Fields virology, 3rd ed. Lippincott-Raven Publishers, Philadelphia, Pa.
19. **Hangartner, L.** 1998. Development of measles virus as a vector. Diploma thesis. University of Zurich, Zurich, Switzerland.
20. **Huber, M., R. Cattaneo, P. Spielhofer, C. Orvell, E. Norrby, M. Messerli, J. C. Perriard, and M. A. Billeter.** 1991. Measles virus phosphoprotein retains the nucleocapsid protein in the cytoplasm. Virology **185:**299–308.
21. **Jansen, A. S. P., X. V. Nguyen, V. Karpitskiy, T. C. Mettenleiter, and A. D. Loewy.** 1995. Central command neurons of the sympathetic nervous system: basis of the fight-or-flight response. Science **270:**644–646.
22. **Kucera, P., M. Dolivo, P. Coulon, and A. Flamand.** 1985. Pathways of the early propagation of virulent and avirulent rabies strains from the eye to the brain. J. Virol. **55:**158–162.
23. **Larsen, P. J., L. W. Enquist, and J. P. Card.** 1998. Characterization of the multisynaptic neuronal control of the rat pineal gland using viral transneuronal tracing. Eur. J. Neurosci. **10:**128–145.
24. **Lawrence, D. M. P., C. E. Patterson, T. L. Gales, J. L. D'Orazio, M. M. Vaughn, and G. F. Rall.** 2000. Measles virus spread between neurons requires cell contact but not CD46 expression, syncytium formation, or extracellular virus production. J. Virol. **74:**1908–1918.
25. **Liebert, U. G.** 1997. Measles virus infections of the central nervous system. Intervirology **40:**176–184.
26. **Liebert, U. G., and D. Finke.** 1995. Measles virus infections in rodents. Curr. Top. Microbiol. Immunol. **191:**149–166.
27. **Maisner, A., H.-D. Klenk, and G. Herrler.** 1998. Polarized budding of measles virus is not determined by viral surface glycoproteins. J. Virol. **72:**5276–5278.
28. **Manchester, M., D. S. Eto, and M. B. Oldstone.** 1999. Characterization of the inflammatory response during acute measles encephalitis in NSE-CD46 transgenic mice. J. Neuroimmunol. **96:**201–217.
29. **McKinney, R. A., M. Capogna, R. Dürr, B. H. Gähwiler, and S. M. Thompson.** 1999. Miniature synaptic events maintain dendritic spines via AMPA receptor activation. Nat. Neurosci. **2:**44–49.
30. **McKinney, R. A., D. Debanne, B. H. Gähwiler, and S. M. Thompson.** 1997. Lesion-induced axonal sprouting and hyperexcitability in the hippocampus *in vitro*: implications for the genesis of posttraumatic epilepsy. Nat. Med. **3:**990–996.
31. **Meissner, N. N., and K. Koschel.** 1995. Downregulation of endothelin receptor mRNA synthesis in C6 rat astrocytoma cells by persistent measles virus and canine distemper virus infections. J. Virol. **69:**5191–5194.
32. **Miwa, T., M. Nonaka, N. Okada, S. Wakana, T. Shiroishi, and H. Okada.** 1998. Molecular cloning of rat and mouse membrane cofactor protein (MCP, CD46): preferential expression in testis and close linkage between the mouse *Mcp* and *Cr2* genes on distal chromosome 1. Immunogenetics **48:**363–371.
33. **Mrkic, B., B. Odermatt, M. A. Klein, M. A. Billeter, J. Pavlovic, and R. Cattaneo.** 2000. Lymphatic dissemination and comparative pathology of recombinant measles viruses in genetically modified mice. J. Virol. **74:**1364–1372.
34. **Naim, H. Y., E. Ehler, and M. A. Billeter.** 2000. Measles virus matrix protein specifies apical virus release and glycoprotein sorting in epithelial cells. EMBO J. **19:**3576–3585.
35. **Oldstone, M. B., H. Lewicki, D. Thomas, A. Tishon, S. Dales, J. Patterson, M. Manchester, D. Homann, D. Naniche, and A. Holz.** 1999. Measles virus infection in a transgenic model: virus-induced immunosuppression and central nervous system disease. Cell **98:**629–640.
36. **Radecke, F., P. Spielhofer, H. Schneider, K. Kaelin, M. Huber, C. Dötsch, G. Christiansen, and M. A. Billeter.** 1995. Rescue of measles virus from cloned DNA. EMBO J. **14:**5773–5784.
37. **Rall, G. F., M. Manchester, L. R. Daniels, A. R. Belman, and M. B. Oldstone.** 1997. A transgenic mouse model for measles virus infection of the brain. Proc. Natl. Acad. Sci. USA **94:**4659–4663.
38. **Rinaman, L., P. Levitt, and J. P. Card.** 2000. Progressive postnatal assembly of limbic-autonomic circuits revealed by central transneuronal transport of pseudorabies virus. J. Neurosci. **20:**2731–2741.
39. **Schneider-Schaulies, J., L. M. Dunster, S. Schneider-Schaulies, and V. ter Meulen.** 1995. Pathogenetic aspects of measles virus infections. Vet. Microbiol. **44:**113–125.
40. **Schneider-Schaulies, S., J. Schneider-Schaulies, L. M. Dunster, and V. ter Meulen.** 1995. Measles virus gene expression in neural cells, p. 101–116. *In* V. ter Meulen and M. A. Billeter (ed.), Measles virus. Springer-Verlag, Berlin, Germany.
41. **Strack, A. M., and A. D. Loewy.** 1990. Pseudorabies virus: a highly specific transneuronal cell body marker in the sympathetic nervous system. J. Neurosci. **10:**2139–2147.
42. **ter Meulen, V., J. R. Stephenson, and H. W. Kreth.** 1983. Subacute sclerosing panencephalitis, p. 105–159. *In* H. Fraenkel-Conrat and R. R. Wagner (ed.), Virus-host interactions: receptors, persistence, and neurological diseases. Plenum Press, New York, N.Y.
43. **Tourtellotte, W. W., J. A. Parker, R. M. Herndon, and C. V. Cuadros.** 1968. Subacute sclerosing panencephalitis: brain immunoglobulin-G, measles antibody and albumin. Neurology **18:**117–121.
44. **Urbanska, E. M., B. J. Chambers, H. G. Ljunggren, E. Norrby, and K. Kristensson.** 1997. Spread of measles virus through axonal pathways into limbic structures in the brain of TAP1−/− mice. J. Med. Virol. **52:**362–369.
45. **Van Pottelsberghe, C., K. W. Rammohan, H. F. McFarland, and M. Dubois-Dalcq.** 1979. Selective neuronal, dendritic, and post-synaptic localization of viral antigen in measles-infected mice. Lab. Investig. **40:**99–108.
46. **Wild, T. F., and R. Buckland.** 1995. Functional aspects of envelope-associated measles virus proteins, p. 51–62. *In* V. ter Meulen and M. A. Billeter (ed.), Measles virus. Springer-Verlag, Berlin, Germany.
47. **Zimmer, J., and B. H. Gähwiler.** 1984. Cellular and connective organization of slice cultures of the rat hippocampus and fascia dentata. J. Comp. Neurol. **228:**432–446.